Uncertainties in the shock devolatilization of hydrated minerals: A nontronite case study

R. G. Kraus,[1,2] S. T. Stewart,[1] M. G. Newman,[1] R. E. Milliken,[3] and N. J. Tosca[4]

[1] Controlled recovery of hydrated minerals subjected to planar shock loading is challenging because of the large difference in shock impedance between the natural samples and the engineering materials used as the recovery capsules. Significant differences in recovery capsule design confound straightforward interpretation of existing data on shock modification of hydrated minerals. We present X-ray diffraction and infrared spectroscopy results from new shock recovery experiments on nontronite (a smectite clay observed on Mars) and identify major issues in the interpretation of recovered samples. Previous work assumes that the first shock pressure step in a ring-up configuration is the most important factor in the interpretation of shock modification. By comparing the X-ray diffraction and infrared spectroscopy data from experiments with similar first shock steps but significantly different final shock states, we show that one cannot simply interpret the recovered samples based upon the first shock pressure step. This work demonstrates the need for a deeper understanding of the thermodynamics of ring-up experiments in order to be able to interpret the results in terms of an equivalent single shock loading pressure for planetary applications. In this work, we also show that venting of the samples does not matter significantly at low pressures but may be important at high pressures. We have developed a recovery method and validation test that allows us to address the major issues and technical tradeoffs with shock recovery experiments on volatile materials.

1. Introduction

[2] Recent detailed observations of hydrated minerals on Mars has rejuvenated interest in understanding the effects of shock processing on major phyllosilicate phases. Understanding the distribution of hydrated minerals in space and time will ultimately constrain paleosurface conditions, providing insight into the evolution of the Martian climate. Phyllosilicates are confined largely to Noachian age terrains [e.g., *Bibring et al.*, 2006; *Ehlmann et al.*, 2013] and thus formed contemporaneously with a period of intense impact cratering. As a result, phyllosilicates may carry an overprint of crustal impact modification. Such pervasive shock processing may have significantly modified or destroyed some phyllosilicates through mechanical and/or thermal processes, which would in turn modify their spectral signatures. Detailed interpretation of the origin(s) and modification of phyllosilicate deposits requires an understanding of the effects of shock modification of the specific phases observed on Mars. Iron-magnesium smectites (nontronite or saponite) are the most common clays identified on Mars, followed by aluminum-rich phases (montmorillonite or kaolinite), chlorite, and serpentine [*Ehlmann et al.*, 2013]. In this work, we conduct shock recovery experiments on nontronite and address key technical issues related to interpreting shock-induced modification of hydrated minerals.

[3] Despite previous experimental attempts aimed at understanding shock-induced structural and spectroscopic changes of phyllosilicates, the data are sparse and difficult to interpret. Part of the difficulty in interpreting the experimental results stems from the significant differences between laboratory shock conditions and planetary impact events and differences between laboratory experimental designs. The differences between the laboratory and nature include the duration of shock loading, stepwise (or ring-up) versus single shock loading paths in pressure-volume-temperature space, and confined versus unconfined conditions upon decompression from the shock state. In this work, we examine the importance of the latter two issues by comparing the shock modification of nontronite subjected to different loading paths and under both confined and unconfined decompression.

[1]Department of Earth and Planetary Sciences, Harvard University, Cambridge, Massachusetts, USA.
[2]Now at Physics Division, Lawrence Livermore National Laboratory, Livermore,CA, USA.
[3]Department of Geological Science, Brown University, Providence, Rhode Island, USA.
[4]Department of Earth and Environmental Sciences, University of St. Andrews, St. Andrews, UK.

Corresponding author: R. G. Kraus, Physics Division, Lawrence Livermore National Laboratory, PO Box 808, Livermore, CA 94551, USA. (kraus4@llnl.gov)

[4] In standard shock recovery studies, samples are recovered in metal containers that are designed to produce a nearly uniform shock loading history over the entire sample and to confine the sample upon decompression [e.g., *Bourne and Gray III*, 2005]. Because hydrated minerals have lower densities and sound speeds compared to steel, the shock wave reverberates in the sample, leading to a stepwise loading path to the peak shock pressure. A stepwise loading path attains much lower entropy and lower shock temperature compared to single shock loading to the same peak shock pressure. Because most of the entropy is gained in the first shock state, some studies interpret shock-induced modifications in terms of the pressure in the first shock state [e.g., *Tyburczy et al.*, 1990] or in terms of the total $\int PdV$ work [*Bowden et al.*, 2000; *DeCarli et al.*, 2002; *Prescher et al.*, 2011] for comparison to single shock states in natural impact events. However, other studies interpret their results in terms of the peak shock pressure without reporting the loading path. The difficulties of interpreting the results in terms of the peak shock stress have been sufficiently discussed by *DeCarli et al.* [2002]. However, the validity of interpreting shock modification in terms of the first shock step or the total energy deposited has not been demonstrated.

[5] In many studies of volatile-bearing phases, above a material-dependent threshold shock pressure, the capsules burst due to expansion of gases upon decompression [e.g., *Weldon et al.*, 1982; *Skala et al.*, 2002; *Zhang and Sekine*, 2007], often preventing successful recovery of the sample. *Ivanov et al.* [2002] calculated the equilibrium isentropic decompression path of carbonate and found that devolatilization requires expansion to multiple orders of magnitude times the original volume. In recognition of the need for volume expansion to study devolatilization, various capsule designs have incorporated vent holes from the sample. In most cases, these vents close during the passage of the shock through the recovery container [*Ivanov et al.*, 2002]. Unfortunately, the incorporation of vent holes in the recovery capsule often has the undesirable side effect of introducing heterogeneous shock loading of the sample. The need for volume expansion upon release is thus a serious technical issue in shock devolatilization studies.

[6] Previous work has found that shock processing can change the near- and mid-infrared spectra of nontronite and other phyllosilicates [*Boslough et al.*, 1980; *Gavin et al.*, 2013; *Sharp et al.*, 2012]: e.g., the O-H stretching modes in the ~3 μm region and Si-O vibration bands at approximately 9 and 20 μm. In general, the O-H stretch feature is diminished and the Si-O vibrational bands are completely removed and replaced by a less distinct glassy spectrum as the shock pressure increases. These spectral changes with increasing pressure were interpreted to be a result of the (1) loss of interlayer and bound water, (2) collapse of the interlayer structure in smectites, and (3) at the highest pressures, shock-induced amorphization.

[7] In this work, we discuss some of the differences between laboratory recovery experiments on clays and impact cratering. We present new shock recovery experiments on nontronite using a novel capsule design to allow for volume expansion while maintaining a simple loading history in the sample. The recovery experiments were designed to illustrate the importance of the recovery fixture itself on the results of the experiment. To better understand the states reached during the recovery experiments, we present measurements of the principal Hugoniot for the nontronite clay used in this study. Finally, we caution against simple interpretations of shock recovery experiments and make suggestions for future experimental designs that would reduce the difficulty in comparing natural impacts to laboratory experiments.

1.1. Previous Shock Modification Studies on Nontronite

[8] Boslough and colleagues conducted two impact shock recovery experiments on nontronite that reached peak pressures of about 18 and 30 GPa [*Boslough et al.*, 1980; *Weldon et al.*, 1982]. The samples were placed in a steel recovery chamber with downrange steel plates backing the sample followed by an enclosed expansion volume. The nontronite samples, from Riverside, California, were powdered and pressed to a density of 2.7 g cm^{-3}. They found that the basal layer collapsed from 14.9 to 11.7 Å and that some of the bound OH was lost in the 30 GPa experiment. In their experimental configuration, the downrange expansion volume led to a second shock loading of the sample upon striking the downrange wall of the recovery chamber. The effects of the second loading event were not considered in the analysis. In a subsequent study, *Boslough et al.* [1986] conducted a series of explosively driven shock recovery experiments (13 to 48 GPa peak pressures) on 37% to 62% porous nontronite in unvented copper fixtures to measure magnetic properties, X-ray diffraction (XRD), and Mössbauer spectroscopy. These experiments suffered from severe heterogeneity in the shock pressure across the sample. In two cases, their capsules ruptured and the results were different than for the enclosed samples, but the details of the differences were not discussed.

[9] More recently, *Gavin et al.* [2013] collected a wide range of spectroscopic data on shock recovered clays, including nontronite. Their experiments utilized a sealed recovery capsule, which ruptured at the highest impact velocity and generated nonplanar loading conditions: a 4×1 mm steel flyer on a 7×4.5 mm polycarbonate sabot impacting a 100×20 mm recovery capsule with a centered 6×5 mm sample located 5 mm from the impact plane (all dimensions are cylindrical diameter × thickness). The samples were pressed powders with unreported densities. The relative dimensions of the projectile and capsule led to highly heterogeneous shock pressure histories in the samples that were estimated by modeling the laboratory experiments using an estimated Hugoniot for the sample. In nontronite, samples subjected to estimated peak pressures of 5.4–17.5 GPa and average shock pressures of 0.9–1.6 GPa did not exhibit any significant changes in the near-infrared spectra but did have changes in the mid-infrared. *Gavin et al.* [2013] also note that the recovered samples exhibit a greater degree of modification than samples studied during heating-only experiments [*Gavin and Chevrier*, 2010], where the predicted postshock temperature from the shock experiments are significantly less than the heating experiments. However, these experiments are extremely difficult to interpret because of the combined problems of heterogeneous, nonplanar shock loading, venting at the highest pressure, and unknown Hugoniot of the sample.

Table 1. Summary of Nontronite Hugoniot Data[a]

Experiment	ρ_0 (g cm^{-3})	V_{imp} (km s^{-1})	U_s (km s^{-1})	u_p (km s^{-1})	P (GPa)	ρ_1 (g cm^{-3})
80	2.03 ± 0.08	1.229 ± 0.015	2.01 ± 0.09	0.60 ± 0.02	2.47 ± 0.16	2.90 ± 0.26
82	2.20 ± 0.02	2.078 ± 0.013	3.34 ± 0.14	0.88 ± 0.02	6.45 ± 0.32	2.98 ± 0.21
85	2.15 ± 0.02	2.268 ± 0.005	3.92 ± 0.12	1.88 ± 0.01	15.83 ± 0.52	4.13 ± 0.28
86	2.16 ± 0.02	2.551 ± 0.008	4.63 ± 0.15	2.06 ± 0.01	20.60 ± 0.70	3.89 ± 0.26
89	2.14 ± 0.02	1.116 ± 0.009	2.64 ± 0.06	0.97 ± 0.01	5.48 ± 0.01	3.38 ± 0.14
90	2.14 ± 0.03	1.024 ± 0.050	3.15 ± 0.05	0.87 ± 0.00	5.85 ± 0.13	2.96 ± 0.09
93	2.17 ± 0.02	1.881 ± 0.006	3.88 ± 0.14	1.55 ± 0.01	13.10 ± 0.50	3.62 ± 0.27

[a]Where ρ_0 is the initial density of the samples, V_{imp} is the measured flyer plate impact velocity, U_s is the measured shock velocity in the sample, u_p is the impedance matched particle velocity, P is the shock pressure, and ρ_1 is the shocked density.

[10] *Sharp et al.* [2012] conducted a series of controlled planar shock recovery experiments on clays in an unvented stainless steel recovery cell. They recovered samples of nontronite that achieved peak pressures ranging from about 10 to 40 GPa. They observe increasing modification to the visible and infrared reflectance spectrum with increasing peak shock pressure [*Friedlander et al.*, 2012] and a broadening of the peaks in the X-ray diffraction spectrum leading to amorphization during the experiment that achieved a ~40 GPa peak shock state.

2. Shock Experiments on Nontronite

[11] We conducted shock Hugoniot measurements and shock recovery experiments on the Harvard 40 mm single stage gun [*Stewart*, 2004]. The nontronite samples were the American Petroleum Institute Clay Mineral Standards H-33a and H-33b from the Lockwood Siding road cut, Manito, Washington.

[12] In most shock recovery experiments on clays, the effects of the shock are presented as a function of peak shock pressure within the recovery cell [e.g., *Sharp et al.*, 2012; *Gavin et al.*, 2013]. The decision to present the recovery data against peak shock pressure is often necessitated by the uncertainty in the Hugoniot of the clay sample, and hence, uncertainty in the first shock step in the shock reverberation. In this work, we measured the Hugoniot of the nontronite clay used in our shock recovery experiments to be able to determine the shock loading path in the metal recovery cells.

2.1. Hugoniot Measurements

[13] The nontronite samples were powdered, sieved to less than 65 μm, and pressed to an average density of 2.14 ± 0.06 g cm^{-3}. Impact velocities from 1.3 to 2.6 km s^{-1} with aluminum or steel flyers generated shock pressures from 2.5 to 23 GPa in the nontronite clay. In experiments 80 and 82, shock velocities were measured by transit times between multiple embedded magnetic particle velocity gauges [*Dremin and Adadurov*, 1964; *Dremin and Shvedov*, 1964; *Petersen et al.*, 1970; *Sheffield et al.*, 2006]. In experiments 85–93, shock velocities were determined by using the relative transit time between two samples of different thickness. A multibeam velocity interferometer system for any reflector [*Barker and Hollenbach*, 1972] or piezoelectric pins was used to determine the time that the shock wave reached the free surface. Piezoelectric pins were also applied to the driver plate to determine the tilt of the flyer

at impact, which was then used to correct the transit times where appropriate. We impedance matched the shocked nontronite sample to the polycarbonate driver (experiments 80 and 82) or the stainless steel driver (experiments 85–93) assuming that the release path of the driver is described by the reflected Hugoniot, which is an accurate approximation for the relatively low pressures achieved in this study.

[14] To determine the Hugoniot of the polycarbonate drivers for the purposes of impedance matching, we combined the Hugoniot data sets of *Millett and Bourne* [2006] with those of *Marsh* [1980] and fit the shock velocity versus particle velocity, U_s-u_p, data below a particle velocity of 1 km s^{-1} with a linear function. Above 1 km s^{-1} particle velocity, the data deviate significantly from the low pressure linear fit. To impedance match to polycarbonate to higher pressures, one should use a higher order polynomial fit to account for the change in slope. Below a particle velocity of 1 km s^{-1}, the polycarbonate Hugoniot is well fit by

$$U_s = 2.00(0.11) + 2.09(16)u_p, \qquad (1)$$

where the correlation coefficient between the intercept and slope is –0.93498, the velocities are in km s^{-1}, and the initial density is $\rho_0 = 1.196$ g cm^{-3}. To impedance match to the stainless steel driver, we used the Hugoniot for SS-304 from *Duffy and Ahrens* [1997].
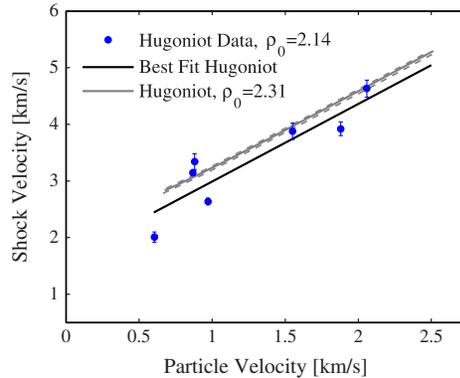
Figure 1. Principal Hugoniot of nontronite pressed powder with an average initial density of 2.14 ± 0.06 g cm^{-3}. Also shown is the best fit Hugoniot (black) and the Hugoniot of nontronite corrected for an initial density of 2.31 g cm^{-3} using a Mie-Grüneison equation of state (gray).
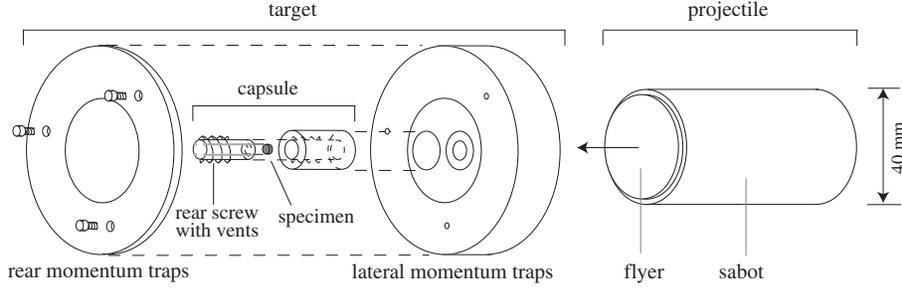
Figure 2. Schematic of a typical target configuration for a shock recovery experiment where two off-axis samples are shocked simultaneously, modified from *Louzada et al.* [2010]. The disc-shaped specimens are positioned 1.5 mm from the impact surface. Samples are set off-axis to avoid stress concentrations on the center line. Lateral and rear momentum traps prevent pressure excursions after the primary shock wave. In a subset of these experiments, the sample capsule was vented by four grooves that are approximately 0.5 mm in depth down the entire length of the rear screw holding the specimen in place. The grooves were sufficiently small to avoid heterogeneous loading of the sample during the ring-up of the sample, however, these grooves closed during the experiments, limiting the possible venting.

[15] The Hugoniot data for nontronite and best fit are presented in Table 1 and in Figure 1. Over this particle velocity range, the linear fit is

$$U_s = 1.62(9) + 1.37(8)u_p, \tag{2}$$

where the correlation coefficient between the intercept and slope is –0.9368. In Figure 1, note the large range of shock velocities near particle velocities of $\sim$0.9 km s^{-1}. The scatter is not a result of a systematic difference in the shock velocity measurement techniques as both the embedded magnetic gauge method and the multisample transit time method produced a relatively high and low shock velocity point in this region of the Hugoniot. The reason for this feature on the Hugoniot is not known.

[16] In general, the intercept of the U_s-u_p fit is the bulk sound velocity in the material. In this work, we measured the longitudinal and transverse sound velocity of the nontronite samples at a density of 2.14 ± 0.02 g cm^{-3} and find the longitudinal, shear, and bulk sound velocities to be 1.47(2), 0.99(5), and 0.93(8) km s^{-1}, respectively. The measured bulk sound velocity is significantly lower than the intercept of a linear fit to the U_s-u_p data. A difference between the measured bulk sound speed and intercept of the linear fit to U_s-u_p data is not unexpected for porous or heterogeneous materials due to the crush-up of pore space and modified grain-grain interactions.

[17] While there are significant residuals, our U_s-u_p data for nontronite are nearly identical to the Hugoniot for a "green deep-lying clay" with low water content studied by *Al'tshuler and Pavlovskii* [1971]: $U_s = 1.6 + 1.47u_p$. While the clay studied by *Al'tshuler and Pavlovskii* [1971] is not positively identified as nontronite, the description, density ($\rho_0 = 2.15$ g cm^{-3}), and similar Hugoniot lends confidence to the Hugoniot measurements obtained in this study.

3. Shock Recovery Experiments

[18] Two specimens of nontronite were shocked simultaneously in recovery capsules made of either stainless steel (SS-304) or aluminum (Al-2024). The recovery capsule design, shown in Figure 2, includes both lateral and rear momentum traps to minimize late time reflections of the shock wave from the free surfaces of the recovery capsule.

[19] The nontronite samples were powdered, sieved to less than 65 μm, baked at 95°C to remove adsorbed water on the surface of the nontronite particles, and pressed to a density of 2.30 ± 0.05 and 2.32 ± 0.08 g cm^{-3} in 8×2 mm discs within the steel and aluminum recovery cells, respectively. The recovery samples could be pressed to higher density than the Hugoniot samples because of their smaller diameter. This pressed density of 2.31 g cm^{-3} is within 2% of the crystal density of nontronite. At the relatively low pressures considered here, the mechanical (P, V, U_s, and u_p) variables on the Hugoniot are not strongly affected by the $\sim$ 9% porosity in the nontronite samples used for the Hugoniot measurements; however, the temperature and entropy along the Hugoniot is sensitive to the starting porosity. Consequently, we attempted to reach the crystal density in the nontronite samples used in the recovery experiments to more accurately match the shock temperature and entropy of natural samples.

3.1. Mie-Grüneisen Hugoniot Correction

[20] To accurately determine the first-step shock pressure in the recovered nontronite samples, we account for the lower porosity in the recovered samples by developing a correction to the Hugoniot of porous nontronite using a Mie-Grüneisen equation of state. Here we assume a value of 1.2 for the Grüneisen parameter, which is consistent with K_0'=4 [*Vocadlo et al.*, 2000], and that the Grüneisen parameter varies inversely with the density. In Figure 1, the corrected Hugoniot is shown in gray with the dashed gray lines representing an illustrative 50% variation in the Grüneisen parameter about $\gamma_0 = 1.2$. Over the particle velocity range of interest, 0.5 to 2.5 km s^{-1}, the effect of the porosity correction is to systematically increase the shock velocity by 5 ± 1%. Below is the corrected Hugoniot of nontronite clay with an initial density of 2.31 g cm^{-3},

$$U_s = 1.88 + 1.35u_p, \tag{3}$$

assuming that the Grüneisen parameter at 2.14 g cm^{-3} is 1.2 and varies inversely with density.
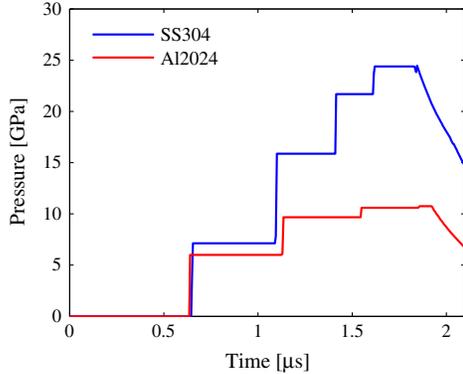
Figure 3. Model pressure histories within the center of the nontronite samples for recovery experiments using the steel (SS304) and aluminum (Al2024) recovery cells. The shock pressure in the sample is released by the rarefaction wave from the rear of the flyer plate.

3.2. Shock Pressure History

[21] The impact velocities for the aluminum and steel recovery fixture were designed so that the first-step shock pressure, and hence peak temperature, would be approximately equal. However, the peak shock pressure is much higher in the steel capsule. The stainless steel recovery fixture was impacted at 1.211 ± 0.005 km s^{-1} by a steel flyer. Using the Hugoniot for stainless steel [*Duffy and Ahrens*, 1997] and our Hugoniot for nontronite, equation (3), we find the first-step shock pressure in the nontronite to be 7.6 ± 0.2 GPa and the peak shock stress after ring-up in the steel to be 26.1 ± 0.2 GPa. The aluminum recovery fixture was impacted at 1.293 ± 0.006 km s^{-1} by an aluminum flyer. Using the Hugoniot for aluminum (Al-2024) (fit presented in *Duffy and Ahrens* [1997]) and our measured Hugoniot for nontronite, we find the first-step shock pressure in the nontronite to be 6.4 ± 0.2 GPa and the peak shock stress after ring-up in the aluminum to be 11.2 ± 0.1 GPa. The impact parameters and shock pressure histories in each experiment are shown in Table 2. The uncertainty in the first-step shock pressure is dominated by the uncertainty in the measured nontronite Hugoniot; the contribution to the uncertainty in the first-step shock pressure by a 50% variation in the Grüneison parameter is $\sim$1%.

[22] Using the CTH shock physics code [*McGlaun et al.*, 1990], we modeled the pressure history within the center of the nontronite samples, shown in Figure 3. To model the nontronite, we used a Mie-Grüneisen equation of state [*Asay and Shahinpoor*, 1993] derived from the Hugoniot measurements and again an assumed value for the Grüneisen parameter of 1.2. For the stainless steel recovery cell, we use the Sesame 4272 tabular equation of state [*Lyon and Johnson*, 1992], and for the aluminum recovery cell, we used the Sesame 3700 equation of state [*Lyon and Johnson*, 1992]. Both tables accurately represent the Hugoniot and reshock states within the pressure range investigated. One can see that the first-step shock pressures achieved were very close in magnitude, within 15% of each other, while the peak shock stress in the steel recovery cell was greater than in the aluminum by more than a factor of 2. If the postshock devolatilization of nontronite is solely driven by the entropic contribution to the Gibbs free energy, as opposed to a change in bonding sites, then we would expect these recovery experiments to show qualitatively similar results as most of the entropy generated during a ring-up experiment occurs during the first shock step.
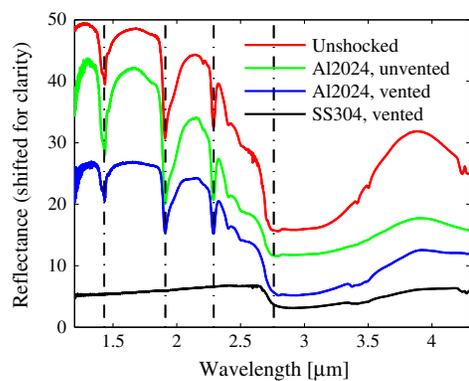
3.3. Venting the Sample

[23] Another difference that has been thought to be important in some studies [*Skala et al.*, 2002] is whether the sample is allowed to release into vacuum, hereafter called vented, or if it is contained within the recovery fixture over the entire release path to ambient pressure and temperature, hereafter unvented. The unvented samples may not follow an isentropic release path as the recovery cell may conduct heat across the sample-recovery cell interface during the decompression process, thereby changing the entropy of the sample and the thermodynamic drive for devolatilization. For the timescale of the experiment, $\sim$1 μs, and a reasonable thermal diffusivity of a rock, $\sim 10^{-7}$ m^2 s^{-1}, the thermal diffusion length scale during the decompression process is of order 1 μm, which suggests a negligible mass of nontronite will be affected by thermal conduction from the steel or aluminum recovery cell during the decompression process. *Boslough et al.* [1980] considered the possibility that the postshock temperature of the recovery cell was sufficient to devolatilize the sample prior to the experimenter removing the nontronite from the cell, over a timescale of tens of minutes. However, as was concluded by *Boslough et al.* [1980], the postshock temperature of the aluminum and steel recovery cells would be approximately 130°C and 200°C [*Raikes and Ahrens*, 1979], respectively, which is insufficient to devolatilize bound OH from nontronite [*Frost et al.*, 2002].

[24] To test the effect of venting on devolatilization, we reduced the thickness of one of the nontronite samples in the aluminum recovery cell to 1 mm and increased the thickness of the corresponding aluminum capsule face, from 1.5 to 2.5 mm, which decreased the plastic strain caused by the differential compression of the nontronite and the recovery cells and so did not fracture during the compression and release process. In the stainless steel recovery experiment, grooves to vent the sample capsule were also machined to

Table 2. Summary of Shock States for the Recovered Nontronite Samples[a]

Recovery Cell	ρ_0 (g cm^{-3})	V_{imp} (km s^{-1})	P_1 (GPa)	P_F (GPa)
Al-2024	2.32 ± 0.08	1.293 ± 0.006	6.4 ± 0.2	11.2 ± 0.1
SS-304	2.30 ± 0.05	1.211 ± 0.005	7.6 ± 0.2	26.1 ± 0.2

[a]Where ρ_0 is the initial density of the samples, V_{imp} is the measured flyer plate impact velocity, P_1 is the first-step shock pressure in the nontronite sample, and P_F is the peak ring-up pressure in the recovery cell.

Figure 4. Near-infrared reflectance spectra of shocked and unshocked nontronite. The spectra are offset vertically for clarity.

Figure 5. Mid-infrared reflectance spectra of shocked and unshocked nontronite. The spectra are offset vertically for clarity.

~0.5 mm depth down the entire length of the rear screw holding the sample in place, Figure 2; however, it was found that the holes completely closed during the experiment. The capsule face in the stainless steel recovery experiment was 1.5 mm thick with a 2 mm thick nontronite sample, and so the capsule face failed during the compression and release process, allowing the nontronite samples to vent during the decompression process.

4. Analysis of Recovered Samples

4.1. Infrared Reflectance Spectroscopy

[25] A Thermo Nicolet 6700 Fourier transform infrared spectrometer in reflectance mode was used to study the IR-active vibrational spectrum of the shocked and unshocked nontronite clay. In Figure 4, the near-infrared reflectance spectra of the recovered samples are compared with an unshocked sample. The nontronite absorption bands at 1.43, 1.91, 2.28, and 2.76 μm are marked by the dash-dotted vertical black lines. The absorptions near 1.43 μm are caused by both structural OH and molecular H_2O, and the band at 1.91 μm is related to interlayer molecular H_2O [*Gavin et al.*, 2013]. The bands at 2.28 and 2.76 μm are related to the Fe–OH bond. One can see the complete loss of the aforementioned absorption bands in the nontronite sample recovered from the steel recovery cell, whereas very little modification occurs to the nontronite samples recovered from the aluminum recovery cell. In Figure 5, the mid-infrared reflectance spectra of the recovered samples are compared with the unshocked sample. Interestingly, the 6.2 μm feature related to H_2O bending is observed in all samples, even the steel recovery cell experiment. However, this may be in part a result of postrecovery adsorbed H_2O, which is also consistent with the presence of the 3 μm band in the steel recovery experiment.

4.2. X-Ray Diffraction

[26] A Scintag XDS2000 fixed sample position powder diffractometer was used to obtain the X-ray diffraction (XRD) spectrum from the shocked and unshocked nontronite samples, where the samples were presented to the X-ray beam in a randomly oriented state. The X-ray spectrum was obtained over a 2θ range of 2° to 40° with a step size of
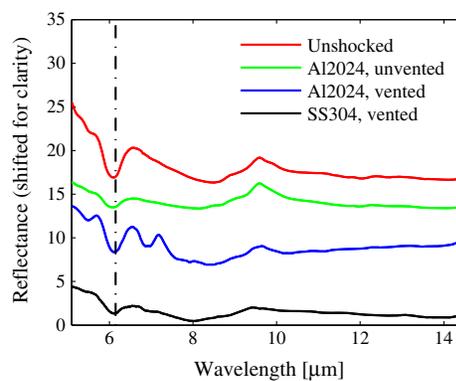
0.02° and at a wavelength of 1.54 Å. In Figure 6, the X-ray diffraction spectra of shocked and unshocked nontronite are compared. The complete loss of scattered intensity from the basal layer, at $2\theta = 6.45$° or ~13.7 Å, and the broad peak at higher scattering angles from the sample recovered from the steel cell suggests amorphization of the nontronite sample. As this is a recovery experiment without temporal resolution, it is not clear whether amorphization occurred during the compression or decompression path; however, it is clear that the X-ray diffraction spectra is significantly different from the nontronite sample recovered from the aluminum cell. For the nontronite sample recovered from the aluminum recovery cell that vented to the chamber during the experiment (blue line in Figure 6), there appears to be no difference between the shocked and unshocked X-ray diffraction spectra.

4.3. Effect of Venting

[27] At an impact velocity of 1.293 ± 0.006 km s^{-1}, we were successful in recovering unvented nontronite from the aluminum capsule with the thicker face and also vented nontronite from the capsule with the thinner face that failed during compression and separated from the recovery cell during decompression. One can see in the infrared reflectance spectroscopy, Figures 4 and 5, that there is very little difference in
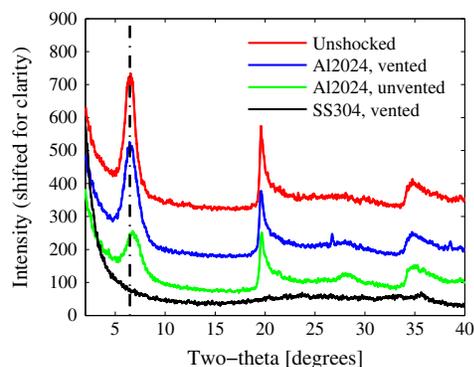
Figure 6. X-ray diffraction spectra of shocked and unshocked nontronite. The spectra are offset vertically for clarity.
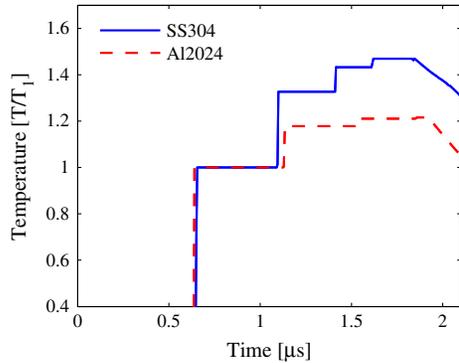
Figure 7. Model temperature histories within the center of the nontronite samples for the recovery experiment using the steel (SS304) and aluminum (Al2024) recovery cells. The temperature histories are normalized to the first-step shock temperature, showing the significantly greater second shock temperature jump in the steel recovery cell than in the aluminum recovery cell. Absolute temperatures were extracted from the CTH shock physics code using a Mie-Grüneison equation of state and a constant specific heat; however, these are not plotted because of the uncertainty in the heat capacity and Grüneison parameter. Shock and postshock temperature measurements are needed.

the molecular and bound water signal. Unexpectedly, there is a slight decrease in the basal layer d-spacing in the unvented sample, while there appears to be no modification to the basal layer in the vented sample, Figure 6. The samples were prepared in an identical manner, and consequently, a significant difference in the preimpact mechanical properties would not be expected.

[28] While we were not able to recover an unvented sample from the highest pressure experiment in the steel recovery cell, we can compare our result with the results of *Boslough et al.* [1980] who were able to recover an unvented sample of nontronite in a stainless steel cell that was impacted at 1.36 km s^{-1}, yielding a peak shock stress of 30.0 GPa. Because of the significantly higher starting density of their nontronite samples, 2.7 g cm^{-3}, which is suggestive of a mineral mixture, we avoid using our measured Hugoniot to compare the first-step shock pressure in the *Boslough et al.* [1980] recovery experiments.

[29] While the peak shock stress in the work by *Boslough et al.* [1980] is slightly higher than that of our experiment, 26.1 GPa, we find starkly different results. *Boslough et al.* [1980] observe a decrease in the basal layer d-spacing from 14.9 to 11.7 Å and that only some of the bound OH was lost in their unvented sample, whereas we observe a complete loss in the basal layer peak and an overall X-ray diffraction spectrum that is suggestive of amorphization in our vented sample. We also observe complete loss of the absorption bands in the near-infrared reflectance spectrum related to bound OH. These results suggest that venting is an important variable in the interpretation of recovered clay minerals at high peak stresses, which is in contrast to the lower peak stress experiment in the aluminum recovery cell where venting does not seem to be important to the interpretation of the shock recovery experiment.

[30] It is possible that the nontronite sample recovered from 30 GPa in the experiment by *Boslough et al.* [1980] was significantly laterally released and hence did not achieve the peak impedance matching pressure in the steel. However, the experiment under consideration used a small sample of nontronite, 16 mg, and is unlikely to have seen the same degree of lateral release as the experiments conducted with much thicker samples. Future experiments will be required to unambiguously determine the effect of venting on the interpretation of these shock recovery experiments.

5. Discussion

5.1. Natural Impacts and Laboratory Experiments

[31] The thermodynamic path taken by a clay sample recovered from a laboratory experiment is significantly different than what would be achieved during a natural impact event [*DeCarli et al.*, 2002]. In the laboratory, one can see in Figure 3 that the pressure increases by a series of steps, with the step height depending on the recovery cell material. The pressure history achieved by a clay sample during a natural impact would be much simpler, a single strong shock wave followed by adiabatic decompression to ambient pressure.

[32] Ignoring the thermal differences created by the path differences, the compressive response of a material can depend on the specific loading path due to the inherent rate dependence of plastic deformation [e.g., *Root and Asay*, 2010]. For nontronite, the path difference between a ring-up and single shock loading could lead to modified criteria for amorphization during compression.

[33] The largest difference in material response between a ring-up, or reverberation, and single shock loading to the same stress is in the thermal state of the material. Because of the lesser amount of work done in compressing the sample to the same pressure, see *Kraus et al.* [2010, Figure 1], the temperature will be significantly lower during a ring-up experiment. It is also not entirely accurate to say that the first-step shock in the ring-up is solely responsible for the temperature and entropy increase. For the pressure states considered in the recovery experiments performed here, Figure 7 presents the relative temperature increase upon ring-up in a steel and aluminum recovery cell. One can see that the second-step shock temperature increase is greater than 30% of the first step in the steel, while the maximum shock temperature is over 140% of the first-step shock temperature. This is in contrast to a ring-up in an aluminum recovery cell where the second-step shock temperature increase is just under 20% of the first-step shock temperature increase, with only an additional few percent increase in temperature to the peak stress state. For comparison, the shock temperature increase upon single shock loading to the peak stress state in the steel (26.1 GPa) and aluminum (11.1 GPa), as in a natural impact event, would be ~4.5 and ~2 times greater than the first-step ring-up temperature increase and ~3.2 and ~1.6 times greater than the maximum temperature increase achieved in the ring-up experiments, respectively. Consequently, the thermal state achieved during a ring-up experiment depends sensitively on the type of recovery cell, for a given peak stress. And in general, ring-up experiments at high shock stresses do a very poor job of simulating the thermal state achieved during a natural impact event.

5.2. Recommendations for Future Clay Recovery Experiments

[34] As there are currently no shock or postshock temperature measurements on nontronite, it is difficult to interpret the absolute thermal history during the ring-up experiment; this is why we have presented the model temperatures as ratios, which are relatively insensitive to the absolute value of the heat capacity. Until such temperature measurements become available, it will be important to experimentally simulate the loading path achieved in a natural impact event in order to be confident that the laboratory experiments mimic nature, while acknowledging the timescale differences between the laboratory and natural events *DeCarli et al.*, [2002].

[35] The closest impedance matched structural material to the clay used in this study is polychlorotrifluoroethylene, with trade name Kel-F. Kel-F is a high density thermoplastic with a well-characterized Hugoniot up to 80 GPa [*Marsh*, 1980],

$$U_s = 2.03 + 1.64u_p, \tag{4}$$

where the velocities are in km s^{-1} and the initial density is $\rho_0 = 2.122$ g cm^{-3}. Nontronite contained in a recovery cell made from Kel-F that is impacted at 2.7 km s^{-1} would reach a first-step shock pressure 11.4 GPa, which is ~94% of the peak ring-up stress, and a temperature that increases by only a few percent after the first-step shock. However, with a low impedance recovery cell, one cannot reach the same peak stresses as with a higher impedance recovery cell, such as steel, and one must also be sure to remove the recovered nontronite clay rapidly from the recovery cell, as the postshock temperature in the Kel-F recovery cell could be sufficient to devolatilize the clay. Another aspect about using Kel-F in a recovery cell is that it has approximately a factor of 10 lower tensile strength than steel, and so the recovery cell would have to be redesigned so that it is not disrupted entirely during the shock wave experiment.

6. Conclusion

[36] Here we measured the principal Hugoniot of nontronite, a smectite clay, over a stress range of 2 to 23 GPa. While there is significant scatter in the individual Hugoniot points, the best fit Hugoniot is in excellent agreement with a green clay measured by *Al'tshuler and Pavlovskii* [1971].

[37] The measured Hugoniot of nontronite was used to interpret the loading history of two shock recovery experiments. One of the experiments used a stainless steel recovery system and the other an aluminum recovery system. The impact velocities were chosen so that the first-step shock pressures were similar; however, they would have a significantly different peak shock stress. We successfully recovered samples of nontronite shocked to a peak stress of 26.1 GPa in the steel and 11.2 GPa in the aluminum, with first-step shock pressures of 7.1 and 6.1 GPa, respectively. Based on near- and mid-infrared reflectance spectroscopy and X-ray diffraction, we found significantly different results between the samples recovered in the steel and aluminum recovery cells, which suggests that one cannot solely use the first-step shock pressure to interpret these types of shock recovery experiments. This statement is especially true for steel and other high impedance recovery cells;

because of the large difference in impedance between the nontronite and steel recovery cell, the second-step shock increases the temperature, and hence entropy, of the nontronite by a significant fraction of the peak ring-up state. Consequently, for shock recovery experiments that depend on the thermal and not just the mechanical state achieved, it is extremely important to both know the pressure history in the sample and mitigate the effects of secondary wave reflections by impedance matching the sample to the recovery cell.

[38] The effect of venting on the devolatilization of nontronite was tested in both recovery experiments. For the aluminum recovery system, one of the nontronite samples vented to the chamber during the experiment and the other was contained for the duration of the experiment. Very little difference was found between the vented and the unvented sample for the specific stress history achieved in the aluminum recovery cell. At significantly higher peak stresses, the vented nontronite sample recovered in these experiments could be compared to the unvented sample recovered in the work of *Boslough et al.* [1980]. A significant difference was found, with the vented sample appearing to amorphize and lose all spectral and XRD signatures of being a well-crystalline clay mineral and the unvented sample showing only some loss of interlayer H_2O and bound OH. However, because of the uncertain loading history in the unvented sample recovered by *Boslough et al.* [1980], more work is needed to determine the significance of venting at high peak stresses.

[39] Given the state of our understanding of how nontronite behaves during shock compression experiments, any inferences made about the shock modification of phyllosilicates on Mars will have significant and unquantified uncertainties.

References

Al'tshuler, L. V., and M. N. Pavlovskii (1971), Response of clay and clay shale to heavy dynamic loading, *J. Appl. Mech. Tech. Phys.*, *1*, 161–165.

Asay, J., and M. Shahinpoor (1993), *High-Pressure Shock Compression of Solids*, Springer-Verlag, New York.

Barker, L. M., and R. E. Hollenbach (1972), Laser interferometer for measuring high velocities of any reflecting surface, *J. Appl. Phys.*, *43*, 4669–4675, doi:10.1063/1.1660986.

Bibring, J. P., et al. (2006), Global mineralogical and aqueous Mars history derived from OMEGA/Mars express data, *Science*, *312*(5772), 400–404, doi:10.1126/science.1122659.

Boslough, M. B., E. L. Venturini, B. Morosin, R. A. Graham, and D. L. Williamson (1986), Physical-properties of shocked and thermally altered nontronite—Implications for the Martian surface, *J. Geophys. Res.*, *91*(B13), E207–E217.

Boslough, M. B., R. J. Weldon, and T. J. Ahrens (1980), Impact-induced water loss from serpentine, nontronite and kernite, in *Proceedings of the 11th Lunar and Planetary Science Conference,* vol. 3, pp. 2145–2158, Pergamon Press, New York.

Bourne, N. K., and G. T. Gray III (2005), Computational design of recovery experiments for ductile metals, *P. Roy. Soc. A-Math. Phy.*, *461*(2062), 3297–3312.

Bowden, E., K. Kondo, T. Ogura, A. P. Jones, G. D. Price, and P. S. DeCarli (2000), *Loading path effects on the shock metamorphism of porous quartz*, Lunar and Planetary Science Conference, vol. 31, Abstract 1582.

DeCarli, P. S., E. Bowden, A. P. Jones, and G. D. Price (2002), Laboratory impact experiments versus natural impact events, *Geol. S. Am. S.*, *356*, 595–605, doi:10.1130/0-8137-2356-6.595.

Dremin, A. N., and G. A. Adadurov (1964), The behavior of glass under dynamic loading, *Sov. Phys.-Sol. State*, *6*(6), 1379–1384.

Dremin, A. N., and K. K. Shvedov (1964), Estimation of Chapman-Jouget pressure and time of reaction in detonation waves of powerful explosives, *J. Appl. Mech. Tech. Phys.*, *2*, 154–159.

Duffy, T. S., and T. J. Ahrens (1997), Dynamic compression of an Fe-Cr-Ni alloy to 80 GPa, *J. Appl. Phys.*, *82*, 4259–4269.

Ehlmann, B. L., G. Berger, N. Mangold, J. R. Michalski, D. C. Catling, S. W. Ruff, E. Chassefière, P. B. Niles, V. Chevrier, and F. Poulet (2013), Geochemical consequences of widespread clay mineral formation in Mars ancient crust, *Space Sci. Rev.*, *174*(1-4), 329–364.

Friedlander, L. R., T. Glotch, J. R. Michalski, T. G. Sharp, M. D. Dyar, and D. L. Bish (2012), *Spectroscopic studies of nontronite after impacts at 3 pressures*, Lunar and Planetary Science Conference, vol. 43, Abstract 2520.

Frost, R. L., J. T. Kloprogge, and Z. Ding (2002), The Garfield and uley nontronites—An infrared spectroscopic comparison, *Spectrochim. Acta, Part A.*, *58*(9), 1881–1894, doi:10.1016/S1386-1425(01)00638-2.

Gavin, P., and V. Chevrier (2010), Thermal alteration of nontronite and montmorillonite: Implications for the Martian surface, *Icarus*, *208*, 721–734.

Gavin, P., V. Chevrier, K. Ninagawa, A. Gucsik, and S. Hasegawa (2013), Experimental investigation into the effects of meteoritic impacts on the spectral properties of phyllosilicates on Mars, *J. Geophys. Res. Planets*, *118*(1), 65–80, doi:10.1029/2012JE004185.

Ivanov, B. A., F. Langenhorst, A. Deutsch, and U. Hornemann (2002), How strong was impact-induced CO_2 degassing in the cretaceous-tertiary event? Numerical modeling of shock recovery experiments, in *Catastrophic Events and Mass Extinctions: Impacts and Beyond, Special Paper,* vol. 356, edited by C. Koeberl and K. MacLeod, pp. 587–594, Geological Society of America, Boulder, CO.

Kraus, R. G., S. T. Stewart, A. Seifter, and A. W. Obst (2010), Shock and post-shock temperatures in an ice-quartz mixture: Implications for melting during planetary impact events, *Earth Planet. Sci. Lett.*, *289*(1-2), 162–170, doi:10.1016/j.epsl.2009.11.002.

Louzada, K. L., S. T. Stewart, B. P. Weiss, J. Gattacceca, and N. Bezaeva (2010), Shock and static pressure demagnetization of pyrrhotite and implications for the Martian crust, *Earth Planet. Sci. Lett.*, *290*, 90–101.

Lyon, S. P., and J. D. Johnson, (1992), SESAME: The Los Alamos national laboratory equation of state database, *Tech. Rep. LA-UR-92-3407*, Los Alamos National Laboratory, Los Alamos, New Mexico.

Marsh, S. P. (1980), *LASL Shock Hugoniot Data*, University of California Press, Berkeley, California.

McGlaun, J. M., S. L. Thompson, and M. G. Elrick (1990), CTH: A three-dimensional shock wave physics code, *Int. J. Impact Eng.*, *10*(1-4), 351–360, doi:10.1016/0734-743X(90)90071-3.

Millett, J. C. F., and N. K. Bourne (2006), Shock and release of polycarbonate under one-dimensional strain, *J. Mater. Sci.*, *41*, 1683–1690.

Petersen, C. F., W. J. Murri, and M. Cowperthwaite (1970), Hugoniot and release-adiabat measurements for selected geologic materials, *J. Geophys. Res.*, *75*(11), 2063–2072.

Prescher, C., F. Langenhorst, U. Hornemann, and A. Deutsch (2011), Shock experiments on anhydrite and new constraints on the impact-induced SO_x release at the K-Pg boundary, *Meteorit. Planet. Sci.*, *46*(11), 1619–1629.

Raikes, S. A., and T. J. Ahrens (1979), Measurements of post-shock temperatures in aluminum and stainless steel, in *High Pressure Science and Technology,* vol. 2, edited by K. D.Timmerhaus and M. S. Barber, pp. 889–894, Plenum Press, New York.

Root, S., and J. R. Asay (2010), Loading path dependence of inelastic behavior: X-cut quartz, in *Shock Compression of Condensed Matter-2009,* vol. 1195, edited by M. L. Elert et al., pp. 999–1002, American Institute of Physics, Melville, NY.

Sharp, T. G., J. R. Michalski, M. D. Dyar, D. L. Bish, L. R. Friedlander, and T. Glotch (2012), *Effects of Shock Metamorphism on Phyllosilicate Structures and Spectroscopy*, Lunar and Planetary Science Conference, vol. 43, Abstract 2806.

Sheffield, S., R. Gustavsen, and R. Alcon (2006), In-situ magnetic gauging technique used at LANL-method and shock information obtained, in *Shock Compression of Condensed Matter-2000*, edited by M. Furnish, L. Chhabildas, and R. Hixson, pp. 1207–1210, American Institute of Physics, Melville, NY.

Skala, R., J. Ederova, P. Matejka, and F. Horz (2002), Mineralogical investigations of experimentally shocked dolomite: Implications for the outgassing of carbonates, in *Catastrophic Events and Mass Extinctions: Impacts and Beyond, Special Paper,* vol. 356, edited by C. Koeberl and K. G. MacLeod, pp. 571–585, Geological Society of America, Boulder, CO.

Stewart, S. T. (2004), *The Shock Compression Laboratory at Harvard: A New Facility for Planetary Impact Processes,* S. Mackwell, and E. Stansbery (eds), Lunar and Planetary Institute Science Conference, vol. 35, Abstracts 1290.

Tyburczy, J. A., R. V. Krishnamurthy, S. Epstein, and T. J. Ahrens (1990), Impact-induced devolatilization and hydrogen isotopic fractionation of serpentine: Implications for planetary accretion, *Earth Planet. Sci. Lett.*, *98*(2), 245–260.

Vocadlo, L., J. P. Poirier, and G. D. Price (2000), Grüneisen parameters and isothermal equations of state, *Am. Mineral.*, *85*, 390–395.

Weldon, R. J., W. M. Thomas, M. B. Boslough, and T. J. Ahrens (1982), Shock-induced color changes in nontronite—Implications for the Martian fines, *J. Geophys. Res.*, *87*(NB12), 102–114.

Zhang, F. P., and T. Sekine (2007), Impact-shock behavior of Mg- and Ca-sulfates and their hydrates, *Geochim. Cosmochim. Acta*, *71*(16), 4125–4133.